PHYSICAL REVIEW D **86,** 095022 (2012)

Polarized, unpolarized direct CP violation, and single lepton polarization asymmetries of $B \to K^* \ell^+ \ell^-$ decay in Z' model

Ishtiaq Ahmed*

National Centre for Physics and Physics Department, Quaid-i-Azam University, Islamabad 45320, Pakistan

(Received 3 September 2012; published 19 November 2012)

In this work, we study the exclusive channel of flavor changing neutral current transition, i.e., $B \to K^* \ell^+ \ell^-$ in the framework of a family of nonuniversal Z' model. In this model, the Z' boson couplings to the fermions could lead to flavor changing neutral current transition (in standard model, this transition is forbidden at tree level and occur via loop) at tree level. In addition, the off-diagonal elements of these effective chiral Z' couplings can contain new weak phases that provide a new source of CP violation and, therefore, could explain the CP asymmetries in the current high energy colliders. In this context, we have studied the polarized and unpolarized CP violation asymmetries for said decay. These asymmetries are highly suppressed in the standard model but significantly enhanced in Z' model. In addition to the CP violation asymmetries, the single lepton polarization asymmetries are also studied and found to be sensitive to the couplings of the Z' boson. Finally, it is analyzed that all of these asymmetries, which will hopefully be tested at LHC, can serve to probe nonuniversal Z' model; particularly, the accurate measurements of these asymmetries may play a crucial role in extracting the precise values of the coupling parameters of the Z' boson.

DOI: 10.1103/PhysRevD.86.095022 PACS numbers: 13.20.He, 12.60.−i, 13.88.+e

I. INTRODUCTION

The study of rare B meson decays which are induced by the flavor changing neutral currents (FCNC) is a highly interesting research area in flavor physics due to many characteristics. First of all, FCNC transitions are rare due to two reasons: (1) In these transitions the off-diagonal Cabibbo-Kobayashi-Maskawa (CKM) matrix elements are involved, which are very small. (2) These transitions are forbidden at tree level in the standard model (SM) but can occur through the Glashow-Iliopoulos-Maiani mechanism at loop level. FCNC transition is not only helpful to determine the precise values of CKM matrix elements [1,2], but also to provide a stringent testing ground for the SM at loop level. Above all, because of loop structure, the FCNC transitions provide a fertile ground to probe new physics (NP), i.e., the physics beyond the SM. This is because many proposed new physics scenarios predict new particles which are heavy in nature, and as such, their direct detection requires very high energy; but these heavy particles can leave their imprints at low energy by manifesting themselves virtually in the FCNC loop and clearly changing the values of observables from their SM values.

On the other hand, it is a fact that the SM is well tested experimentally and proved to be a successful theory of the twentieth century. Despite many hallmarks of the SM, one cannot consider it as a fundamental theory due to some basic shortcomings such as absence of gravity; 22 free parameters appear in the Yukawa sector of the SM including the masses and mixing angles of particles. Further, why is the CKM matrix hierarchical? Why are the quark masses (except for the top mass) so small compared to the electroweak vacuum expectation value? Why do we have three families? Why is there no CP violation in flavor-diagonal processes? etc. These shortcomings impede the SM becoming a fundamental theory. In addition, during the last few years some mismatches between the SM predictions and experimental measurements have been found [3–7], which is a clear indication of new physics.

To overcome the fundamental shortcomings in the SM and accommodate the experimental measurements with the theory, many models are cooked [8–13]. As mentioned earlier, these models can be checked at low energies in the current hadron colliders through FCNC transitions. In this context, the rare semileptonic FCNC transitions are relatively clean compared to the pure hadronic transition. In particular, $B \to K^* \ell^+ \ell^-$, where $\ell = \mu$, τ has a great interest due to the fact that it has the largest branching ratio among many radiative and other semileptonic rare B meson decays. On the other hand, among the new physics scenarios which are mentioned above, nonuniversal Z' model looks like an attractive extension of the SM (for a detailed review, see Ref. [12]). Like the behavior of the off-diagonal couplings of the nonuniversal Z' boson with the fermions, the FCNC transitions can occur at tree level; this model also helps to resolve the puzzles in the data of rare B meson decays such as the anomaly in the $B_s - \bar{B}_s$ mixing phase [14,15], π-K puzzle [16], etc.

Regarding probing the new physics, the semileptonic decay channels based on the $b \to s$ transitions provide a number of observables such as forward-backward asymmetry, helicity fractions, single and double lepton polarization asymmetries, etc. The measurements of these observables at current colliders may provide useful information to sketch

*ishtiaq@ncp.edu.pk

out the structure of proposed theories beyond the SM. Therefore, to explore the physics beyond the SM, various inclusive B meson decays like $B \to X_{s,d}\ell^+\ell^-$ and their corresponding exclusive processes, like $B \to M\ell^+\ell^-$ with $M = K,\ K^*,\ K_1,\ \rho$, etc. have been investigated in the literature [17–31]. In these studies a large number of observables are examined which showed that the aforementioned inclusive and exclusive decays of B meson are very sensitive to the flavor structure of the standard model and provide a windowpane for any NP model.

Further, the investigation of nonuniversal family coupling of Z' bosons leading to FCNC transitions have also been studied by considering different observables such as branching ratios and forward-backward asymmetry [32,33]. In this context, the behavior of the other observables in the presence of the Z' boson may play a crucial role in refining our knowledge about the family of nonuniversal Z' model. With this motivation we have studied single lepton polarization asymmetries, as well as both polarized and unpolarized CP violation asymmetries, within the SM and in Z' model. In the context of CP asymmetry, it is important to emphasize here that the FCNC transitions are proportional to three CKM matrix elements, namely, $V_{tb}V_{ts}^*$, $V_{cb}V_{cs}^*$, and $V_{ub}V_{us}^*$; however, due to the unitarity condition, and neglecting $V_{ub}V_{us}^*$ in comparison of $V_{cb}V_{cs}^*$ and $V_{tb}V_{ts}^*$, the CP asymmetry is highly suppressed in the SM. Therefore, the measurement of CP violation asymmetries in FCNC processes could provide a key evidence for new physics.

The scheme of this manuscript is as follows. Section II contains the basic theoretical formulation which is necessary to calculate the different physical observables for $B \to K^*\ell^+\ell^-$. In Sec. III, we give the formulas and explicit expressions of observables which are under consideration in this manuscript. In Sec. IV we present the numerical analysis to show how the lepton polarization asymmetries and CP violation asymmetries are influenced due to the contribution of the Z' boson. In the last section, we give our conclusions.

II. THEORETICAL FORMULATION

The decay channel which we are interested in ($B \to K^* l^+ l^-,\ l = \mu,\ \tau$) is the FCNC transition and originates from the quark level transition $b \to s l^+ l^-$. The QCD corrected effective Hamiltonian responsible for the $b \to s l^+ l^-$ transition can be written as follows:

$$H_{\rm eff} = -\frac{4G_F}{\sqrt{2}} V_{tb}^* V_{ts} \sum_{i=1}^{10} C_i(\mu) O_i(\mu), \tag{1}$$

where $O_i(\mu)$ ($i = 1, \ldots, 10$) are the four-quark operators and $C_i(\mu)$ are the corresponding Wilson coefficients at the energy scale μ and the explicit expressions of these Wilson coefficients at next-to-leading order and next-to-next-to-leading order are given in Refs. [34–44]. We have neglected the terms proportional to $V_{ub}V_{us}^*$ because of $\frac{V_{ub}V_{us}^*}{V_{tb}V_{ts}^*} < 0.02$. The operators responsible for $B \to K^*\ell^+\ell^-$ are O_7, O_9, and O_{10} and their form is given by

$$\begin{aligned} O_7 &= \frac{e^2}{16\pi^2} m_b (\bar{s}\sigma_{\mu\nu} P_R b) F^{\mu\nu}, \\ O_9 &= \frac{e^2}{16\pi^2} (\bar{s}\gamma_\mu P_L b)(\bar{l}\gamma^\mu l), \\ O_{10} &= \frac{e^2}{16\pi^2} (\bar{s}\gamma_\mu P_L b)(\bar{l}\gamma^\mu \gamma_5 l), \end{aligned} \tag{2}$$

with $P_{L,R} = (1 \pm \gamma_5)/2$.

Neglecting the mass of the s quark, the above effective Hamiltonian gives the following matrix element:

$$\begin{aligned} &\mathcal{M}(B \to K^* l^+ l^-) \\ &= \frac{\alpha_{em} G_F}{2\sqrt{2}\pi} V_{tb}^* V_{ts} \Big[\langle K^*(k,\epsilon)|\bar{s}\gamma^\mu(1-\gamma^5)b|B(p)\rangle \\ &\quad \times \{C_9^{\rm eff}(\bar{l}\gamma^\mu l) + C_{10}(\bar{l}\gamma^\mu\gamma^5 l)\} \\ &\quad - 2C_7^{\rm eff} m_b \langle K^*(k,\epsilon)|\bar{s} i\sigma_{\mu\nu}\frac{q^\nu}{s}(1+\gamma^5)b|B(p)\rangle(\bar{l}\gamma^\mu l)\Big], \end{aligned} \tag{3}$$

where q is the momentum transfer to the final lepton pair; i.e., $q = p_1 + p_2$, where p_1 and p_2 are the momentum of l^- and l^+, respectively, and s is the square of the momenta transfer. $V_{tb}^* V_{ts}$ are the CKM matrix elements.

The Wilson coefficient $C_9^{\rm eff}$ in Eq. (3) contains a perturbative part $C_9^{\rm per}$ which includes the indirect contributions of operators O_i, where $i = 1$ to 6 to $b \to s$ and a nonperturbative part $C_9^{\rm res}$ which contains the long-distance resonance effects due to conversion of the real $c\bar{c}$ into the lepton pair $l^+ l^-$. Therefore, $C_9^{\rm eff}$ can be written as

$$C_9^{\rm eff} = C_9^{\rm per} + C_9^{\rm res}, \tag{4}$$

where the $C_9^{\rm per}$ is read as [45]

$$\begin{aligned} C_9^{\rm per} &= C_9(m_b) + g(m_c, s)\Big(\frac{4}{3}C_1 + C_2 + 6C_3 + 60C_5\Big) \\ &\quad - \frac{2}{2} g(m_b, s)\Big(7C_3 + \frac{4}{3}C_4 + 76C_5 + \frac{64}{3}C_6\Big) \\ &\quad - \frac{1}{2} g(0, s)\Big(C_3 + \frac{4}{3}C_4 + 16C_5 + \frac{64}{3}\Big) \\ &\quad + \frac{4}{3}C_3 + \frac{64}{9}C_5 + \frac{64}{27}C_6. \end{aligned} \tag{5}$$

Here the functions $g(m_i, s)$ include the one-loop correction to the four-quark operators $O_1, \ldots, O_6$ and have the form [35,45]

$$g(m_i, s) = \frac{8}{27} - \frac{8}{9}\ln(m_i) + \frac{4}{9}y_i - \frac{2}{9}(2 + y_i)\sqrt{|1 - y_i|} \times \begin{cases} \left(\ln\left|\frac{\sqrt{1-y_i}+1}{\sqrt{1-y_i}-1}\right| - i\pi\right), & \text{for } y_i \le 1 \\ 2\arctan\frac{1}{\sqrt{y_i-1}}, & \text{for } y_i > 1, \end{cases}$$

where $y \equiv 4m_i^2/s$. The nonperturbative part $C_9^{\rm res}$ arises from the intermediate states of the real $c\bar{c}$ states and can be parametrized by using the Breit-Wigner formula in the following way:

$$C_9^{\rm res} = -\frac{3\pi}{\alpha^2}\kappa[3C_1 + C_2 + 3C_3 + C_4 + 3C_5 + C_6] \times \sum_{V=\psi} \frac{m_V B_r(V \to l^+l^-)\Gamma^V_{\rm total}}{s - m_V^2 + i m_V \Gamma_{\rm total^V}}. \quad (6)$$

It is worth mentioning here that in the present study, we do not include the long-distance effects in our calculation. As stated in the introduction, due to the presence of off-diagonal couplings in Z' model, FCNC transitions can occur at tree level. In this regard, to reduce the number of parameters, the Z-Z' mixing and the interaction of right-handed quarks with Z' are usually ignored [32]. Therefore, the Z' boson contribution is only to modify the Wilson coefficients C_9 and C_{10}. With these assumptions, the additional part of the effective Hamiltonian due to the Z' contribution can be written as follows [33,46–48]:

$$\mathcal{H}^{Z'}_{\rm eff} = -\frac{2G_F}{\sqrt{2}}\bar{s}\gamma^\mu(1 - \gamma^5)bB_{sb}[\mathcal{S}^L_{\ell\ell}\bar{\ell}\gamma^\mu(1 - \gamma^5)\ell - \mathcal{S}^R_{\ell\ell}\bar{\ell}\gamma^\mu(1 + \gamma^5)\ell] + \text{H.c.}, \quad (7)$$

where B_{sb} is the off-diagonal left-handed coupling of the Z' boson with quarks, and $\mathcal{S}^L_{\ell\ell}$ and $\mathcal{S}^R_{\ell\ell}$ represent the left- and right-handed couplings of the Z' boson with leptons, respectively. It is noted here that if a new weak phase ϕ_{sb} is introduced in the off-diagonal coupling B_{sb}, then this coupling could be read as $B_{sb} = \mathcal{R}e(B_{sb})e^{-i\phi_{sb}}$. Therefore, one can also write the above equation in the following way:

$$\mathcal{H}^{Z'}_{\rm eff} = -\frac{4G_F}{\sqrt{2}}V_{tb}V^*_{ts}[\Lambda_{sb}C_9^{Z'}\mathcal{O}_9 + \Lambda_{sb}C_{10}^{Z'}\mathcal{O}_{10}] + \text{H.c.}, \quad (8)$$

where

$$\Lambda_{sb} = \frac{4\pi e^{-i\phi_{sb}}}{\alpha V^*_{ts}V_{tb}}; \qquad C_9^{Z'} = \mathcal{R}e(B_{sb})S_{LL}; \qquad C_{10}^{Z'} = \mathcal{R}e(B_{sb})D_{LL}; \qquad S_{LL} = \mathcal{S}^L_{\ell\ell} + \mathcal{S}^R_{\ell\ell}; \qquad D_{LL} = \mathcal{S}^L_{\ell\ell} - \mathcal{S}^R_{\ell\ell}. \quad (9)$$

Thus, to include the Z' effects in the problem under consideration, one has to make the following replacements in the Wilson coefficients C_9 and C_{10}, while C_7 remains unchanged:

$$C_9^{\rm tot} = C_9^{\rm eff} + \Lambda_{sb}C_9^{Z'}, \qquad C_{10}^{\rm tot} = C_{10} + \Lambda_{sb}C_{10}^{Z'}. \quad (10)$$

The matrix elements in the $B \to K^*l^+l^-$ decay amplitude in Eq. (3) can be parametrized in terms of the form factors as follows [29,35,42,49–52]:

$$\begin{aligned}\langle K^*(k,\epsilon)|\bar{s}\gamma^\mu(1 \pm \gamma^5)b|B(p)\rangle &= \mp iq_\mu\frac{2m_{K^*}}{s}\epsilon^*\cdot q[A_3(s) - A_0(s)] \pm i\epsilon^*_\mu(m_B + m_{K^*}) \times A_1(s) \mp i(p+k)_\mu\epsilon^*\cdot q\frac{A_2(s)}{(m_B + m_{K^*})} - \epsilon_{\mu\nu\lambda\sigma}p^\lambda q^\sigma\frac{2V(s)}{(m_B + m_{K^*})}. \end{aligned} \quad (11)$$

Contracting above equation by q_μ and using the equation of motion, the form factors $A_3(s)$ can be expressed in terms of the $A_1(s)$ and $A_2(s)$ form factors as follows:

$$A_3(s) = \frac{m_B + m_{K^*}}{2mK^*}A_1(s) - \frac{m_B - m_{K^*}}{2mK^*}A_2(s) \quad (12)$$

and

$$\begin{aligned}\langle K^*(k,\epsilon)|\bar{s}i\sigma_{\mu\nu}q^\nu(1 \pm \gamma^5)b|B(p)\rangle &= 2\epsilon_{\mu\nu\lambda\sigma}p^\lambda q^\sigma F_1(s) \pm i\{\epsilon^*_\mu(m_B^2 - m_{K^*}^2) - (p+k)_\mu\epsilon^*\cdot q\}F_2(s) \pm i\epsilon^* \cdot q\left\{q_\mu - \frac{(p+k)_\mu}{(m_B^2 - m_{K^*}^2)}\right\}F_3(s). \end{aligned} \quad (13)$$

These seven independent form factors [$V(s)$, $A_1(s)$, $A_2(s)$, $A_0(s)$, $F_1(s)$, $F_2(s)$, and $F_3(s)$] are the scalar function of the square of the momentum transfer $s = q^2 = (p - k)^2$ and are nonperturbative quantities. These form factors are the main source of hadronic uncertainties and are calculated by different nonperturbative schemes such as lattice QCD, quark model [53], perturbative QCD, light cone-QCD sum rules [44,54], etc.

By using the matrix elements which are parametrized in terms of the form factors [Eqs. (11) and (13)] with the expression (3), the decay amplitude for $B \to K^*l^+l^-$ can be written as

$$\begin{aligned}\mathcal{M} = \frac{\alpha G_F}{4\sqrt{2}\pi}V^*_{tb}V_{ts}[\bar{l}\gamma^\mu(1 - \gamma^5)l \times (-2\mathcal{A}\epsilon_{\mu\nu\lambda\sigma}\epsilon^*k^\lambda q^\sigma - i\mathcal{B}_1\epsilon^*_\mu + i\mathcal{B}_2\epsilon^*\cdot q(p+k)_\mu + i\mathcal{B}_0\epsilon^*\cdot qq_\mu) + \bar{l}\gamma^\mu(1 + \gamma^5)l \times (-2\mathcal{C}\epsilon_{\mu\nu\lambda\sigma}\epsilon^*k^\lambda q^\sigma - i\mathcal{D}_1\epsilon^*_\mu + i\mathcal{D}_2\epsilon^*\cdot q(p+k)_\mu + i\mathcal{D}_0\epsilon^*\cdot qq_\mu)]. \end{aligned} \quad (14)$$

Here the last term in the first line of the above equation will survive only for $\bar{l}\gamma^\mu\gamma^5 l$ due to the fact that $q_\mu(\bar{l}\gamma^\mu\gamma^5 l) = 2m_l(\bar{l}\gamma^5 l)$ and will vanish for $\bar{l}\gamma^\mu l$ because of $q_\mu(\bar{l}\gamma^\mu l) = 0$. However, the auxiliary functions $\mathcal{A}$, $\mathcal{C}$, $\mathcal{B}_1$, $\mathcal{D}_1$, $\mathcal{B}_2$, $\mathcal{D}_2$, $\mathcal{B}_0$, and $\mathcal{D}_0$ contain both long- and short-distance physics which are encapsulated in the form factors and in the Wilson coefficients, respectively, and can be written in the following form:

$$\mathcal{A} = 2C_{LL}\mathcal{H}_1 + 4m_b C_7^{\rm eff}\frac{F_1(s)}{s}, \qquad \mathcal{B}_1 = 2C_{LL}\mathcal{H}_3 + \frac{4m_b}{s}C_7^{\rm eff}\mathcal{H}_4, \qquad \mathcal{B}_2 = 2C_{LL}\mathcal{H}_6 + 4\frac{m_b C_7^{\rm eff}}{s}\times\mathcal{H}_5,$$
$$\mathcal{B}_0 = \frac{2m_{k^*}}{s}\mathcal{H}_7 - \frac{4m_b}{s}C_7^{\rm eff}F_3(s), \qquad \mathcal{C} = \mathcal{A}(C_{LL}\to C_{LR}), \qquad \mathcal{D}_1 = \mathcal{B}_1(C_{LL}\to C_{LR}), \tag{15}$$
$$\mathcal{D}_2 = \mathcal{B}_2(C_{LL}\to C_{LR}), \qquad \mathcal{D}_0 = \mathcal{B}_0(C_{LL}\to C_{LR}),$$

where

$$C_{LL} = C_9^{\rm tot} - C_{10}^{\rm tot}, \qquad C_{LR} = C_9^{\rm tot} + C_{10}^{\rm tot}, \qquad \mathcal{H}_1 = \frac{V(s)}{(m_B + m_{K^*})}, \qquad \mathcal{H}_3 = (m_B + m_{K^*})A_1(s),$$
$$\mathcal{H}_4 = (m_B^2 - m_{K^*}^2)F_2(s), \qquad \mathcal{H}_6 = \frac{A_2(s)}{(m_B + m_{K^*})}, \qquad \mathcal{H}_5 = \left[F_2(s) + \frac{s}{(m_B^2 - m_{K^*}^2)}F_3(s)\right], \qquad \mathcal{H}_7 = (A_3 - A_0). \tag{16}$$

III. PHYSICAL OBSERVABLES

Now, we have all the ingredients to calculate the physical observables. The double differential decay rate is given in Ref. [28]

$$\frac{d^2\Gamma(B\to K^* l^+ l^-)}{d\cos\theta ds} = \frac{1}{2m_B^3}\frac{2\beta\sqrt{\lambda}}{(8\pi)^3}|\mathcal{M}|^2, \tag{17}$$

where $\beta \equiv \sqrt{1-\frac{4m_l^2}{s}}$ and $\lambda \equiv m_B^4 + m_{k^*}^4 + s^2 - 2m_B^2 m_{k^*}^2 - 2m_B^2 s - 2m_{k^*}^2 s$. By using the expression of the decay amplitude given in Eq. (14), one can get the expression of the dilepton invariant mass spectrum as

$$\frac{d\Gamma(B\to K^* l^+ l^-)}{ds} = \frac{G_F^2\alpha^2\beta\sqrt{\lambda}m_B}{2^{14}\pi^5}|V_{tb}V_{ts}^*|^2\Delta, \tag{18}$$

where

$$\Delta = 4(2m_l^2 + s)\left\{\frac{8\lambda}{3}\mathcal{R}e|\mathcal{A}|^2 + \frac{12m_{K^*}^2 s + \lambda}{3m_{K^*}^2 s}\mathcal{R}e|\mathcal{B}_1|^2 - \frac{(m_B^2 - m_{K^*}^2 - s)}{3m_{K^*}^2 s}\mathcal{R}e(\mathcal{B}_1\mathcal{B}_2^*) + \frac{\lambda}{3m_{K^*}^2 s}\mathcal{R}e|\mathcal{B}_2|^2\right\}$$
$$+ \frac{32\lambda}{3}(s - 4m_l^2)\mathcal{R}e|\mathcal{C}|^2 + \left[\frac{4\lambda(2m_l^2 + s)}{3m_{K^*}^2 s} + 16(s - 4m_l^2)\right]\times\mathcal{R}e|\mathcal{D}_1|^2 - \frac{4\lambda}{3m_{K^*}^2 s}\{[(2m_l^2 + s)(m_B^2 - m_{K^*}^2)$$
$$+ s(s - 4m_l^2)]\mathcal{R}e(\mathcal{D}_1\mathcal{D}_2^*) + [6m_l^2 s(2m_B^2 + 2m_{K^*}^2 - s) + \lambda(2m_l^2 + s)]\mathcal{R}e|\mathcal{D}_2|^2$$
$$+ \frac{8m_l^2\lambda}{m_{K^*}^2}(m_B^2 - m_{K^*}^2)\mathcal{R}e(\mathcal{D}_2\mathcal{D}_0^*) - \frac{8m_l^2\lambda}{m_{K^*}^2}\mathcal{R}e|\mathcal{D}_0|^2. \tag{19}$$

A. Single lepton polarization asymmetries

In this section we will compute the single lepton polarization asymmetries in the $B\to K^* l^+ l^-$, i.e., the asymmetries where only one of the final state leptons is polarized. For this purpose we first define the six orthogonal vectors belonging to the polarization of l^- and l^+, which we denote here by S_i and W_i, respectively, where $i = L, N$, and T, corresponding to the longitudinally, normally, and transversally polarized lepton $l^\pm$, respectively [37,55].

$$S_L^\mu \equiv (0, \mathbf{e}_L^-) = \left(0, \frac{\mathbf{p}_-}{|\mathbf{p}_-|}\right), \qquad S_N^\mu \equiv (0, \mathbf{e}_N^-) = \left(0, \frac{\mathbf{k}\times\mathbf{p}_-}{|\mathbf{k}\times\mathbf{p}_-|}\right), \qquad S_T^\mu \equiv (0, \mathbf{e}_T^-) = (0, \mathbf{e}_N\times\mathbf{e}_L), \tag{20}$$

$$W_L^\mu \equiv (0, \mathbf{e}_L^+) = \left(0, \frac{\mathbf{p}_+}{|\mathbf{p}_+|}\right), \qquad W_N^\mu \equiv (0, \mathbf{e}_N^+) = \left(0, \frac{\mathbf{k}\times\mathbf{p}_+}{|\mathbf{k}\times\mathbf{p}_+|}\right), \qquad W_T^\mu \equiv (0, \mathbf{e}_T^+) = (0, \mathbf{w}_N\times\mathbf{w}_L), \tag{21}$$

where p_+, p_-, and k denote the three momenta vectors of the final particles l^+, l^-, and k, respectively. These polarization vectors $S_i^\mu(W_i^\mu)$ in Eqs. (20) and (21) are defined in the rest frame of $l^-(l^+)$. When we apply a Lorentz boost to bring these polarization vectors from the rest frame of $l^-(l^+)$ to the center of mass frame of final leptons, only the longitudinal polarization four-vector is changed while the other two polarization vectors remain unchanged. After this operation the longitudinal four-vector reads as

$$S_L^\mu = \left(\frac{|p_-|}{m_l}, \frac{E_l \mathbf{p}_-}{m_l|\mathbf{p}_-|}\right), \quad W_L^\mu = \left(\frac{|p_+|}{m_l}, -\frac{E_l \mathbf{p}_+}{m_l|\mathbf{p}_+|}\right). \tag{22}$$

To achieve the polarization asymmetries one can use the spin projectors $\frac{1}{2}(1+\gamma_5 \mathcal{S})$ and $\frac{1}{2}(1+\gamma_5 \mathcal{W})$ for ℓ^- and ℓ^+, respectively. The single lepton polarization asymmetries formula is given in Refs. [55,56]:

$$P_i^\pm = \frac{\frac{d\Gamma(\mathbf{S}^\pm = \mathbf{e}_i^\pm)}{ds} - \frac{d\Gamma(\mathbf{S}^\pm = -\mathbf{e}_i^\pm)}{ds}}{\frac{d\Gamma(\mathbf{S}^\pm = \mathbf{e}_i^\pm)}{ds} + \frac{d\Gamma(\mathbf{S}^\pm = -\mathbf{e}_i^\pm)}{ds}}, \tag{23}$$

where i denotes the L, N and T and $\mathbf{S}^\pm$ is the spin direction of $l^\pm$. The relation between the polarized and unpolarized invariant dilepton mass spectrum for the $B \to K^* l^+ l^-$ reads as

$$\frac{d\Gamma(\mathbf{S}^\pm)}{ds} = \frac{1}{2}\left(\frac{d\Gamma}{ds}\right)[1 + (P_L \mathbf{e}_L^\pm + P_N \mathbf{e}_N^\pm + P_T \mathbf{e}_T^\pm)\cdot \mathbf{S}^\pm]. \tag{24}$$

By using the decay rate which is given in Eq. (18) with the polarization vectors defined in Eqs. (20)–(22), we get the following expressions for the single lepton polarization asymmetries:

$$\begin{aligned} P_L(s) = {} & \frac{16\lambda}{3}\sqrt{s(s-4m_l^2)}\mathcal{R}e(\mathcal{A}\mathcal{C}^*) + \frac{4\sqrt{s-4m_l^2}}{3m_{K^*}^2\sqrt{s}} \\ & \times\{(12m_{K^*}^2 s + \lambda)\times \mathcal{R}e(\mathcal{B}_1\mathcal{D}_1^*) \\ & - \lambda(m_B^2 - m_{K^*}^2 - s)[\mathcal{R}e(\mathcal{B}_1\mathcal{D}_2^*) \\ & + \mathcal{R}e(\mathcal{B}_2\mathcal{D}_1^*)] + \lambda^2 \mathcal{R}e(\mathcal{B}_2\mathcal{D}_2^*)\mathcal{R}e|\mathcal{B}_1|^2\}, \end{aligned} \tag{25}$$

$$\begin{aligned} P_N(s) = {} & \frac{4\pi m_l\sqrt{\lambda}}{\sqrt{s}}\Big\{s\mathcal{R}e(\mathcal{A}\mathcal{B}_1^*) + \frac{(m_B^2 - m_{K^*}^2 - s)}{4m_{K^*}^2} \\ & \times[\mathcal{R}e(\mathcal{B}_1\mathcal{D}_1^*) - (m_B^2 - m_{K^*}^2)\mathcal{R}e(\mathcal{B}_1\mathcal{D}_2^*) \\ & + s\mathcal{R}e(\mathcal{B}_1\mathcal{D}_0^*)]\Big\} - \frac{\lambda}{m_{K^*}^2}\{\mathcal{R}e(\mathcal{B}_2\mathcal{D}_1^*) \\ & + (m_B^2 - m_{K^*}^2)\mathcal{R}e(\mathcal{B}_2\mathcal{D}_2^*) + s\mathcal{R}e(\mathcal{B}_2\mathcal{D}_0^*)\}, \end{aligned} \tag{26}$$

$$\begin{aligned} P_T(s) = {} & 4\pi m_l\sqrt{\lambda(s-4m_l^2)}\Big\{Im(\mathcal{A}\mathcal{D}_1^*) + Im(\mathcal{B}_1\mathcal{C}^*) \\ & + \frac{(m_B^2 + 3m_{K^*}^2 - s)}{4m_{K^*}^2} Im(\mathcal{D}_1\mathcal{D}_2^*) \\ & + \frac{(m_B^2 - m_{K^*}^2 - s)}{4m_{K^*}^2} Im(\mathcal{D}_1\mathcal{D}_0^*) \\ & - \frac{\lambda}{m_{K^*}^2} Im(\mathcal{D}_2\mathcal{D}_0^*)\Big\}. \end{aligned} \tag{27}$$

B. Polarized and unpolarized *CP* asymmetries

The normalized *CP* violation asymmetries can be defined through the difference of the differential decay rates of particle and antiparticle decay modes as follows [57,58]:

$$\mathcal{A}_{CP}(\mathbf{S}^\pm = \mathbf{e}_i^\pm) = \frac{\frac{d\Gamma(\mathbf{S}^-)}{ds} - \frac{d\bar{\Gamma}(\mathbf{S}^+)}{ds}}{\frac{d\Gamma}{ds} - \frac{\bar{\Gamma}}{ds}}, \tag{28}$$

where

$$\frac{d\Gamma}{ds} = \frac{d\Gamma(B \to K^*\ell^+\ell^-(\mathbf{S}^-))}{ds}, \quad \frac{d\bar{\Gamma}}{ds} = \frac{d\bar{\Gamma}(B \to K^*\ell^+(\mathbf{S}^+))\ell^-}{ds}.$$

The differential decay rate of $b \to s\ell^+\ell^-$ is given in Eq. (22); analogously, the *CP* conjugated differential decay width can be written as

$$\frac{d\bar{\Gamma}(\mathbf{S}^\pm)}{ds} = \frac{1}{2}\left(\frac{d\bar{\Gamma}}{ds}\right)[1 + (P_L \mathbf{e}_L^\pm + P_N \mathbf{e}_N^\pm + P_T \mathbf{e}_T^\pm)\cdot \mathbf{S}^\pm]. \tag{29}$$

It is noted here that $\frac{d\bar{\Gamma}}{ds}$ belongs to the transition $\bar{b} \to \bar{s}\ell^+\ell^-$, which can be obtained by replacing Λ_{sb} with Λ_{sb}^* in Eq. (7). Furthermore, by using the fact that $\mathbf{S}^+ = -\mathbf{S}^-$ for L, N and $\mathbf{S}^+ = \mathbf{S}^-$ for T, we get

$$\begin{aligned} & \mathcal{A}_{CP}(\mathbf{S}^\pm = \mathbf{e}_i^\pm) \\ & = \frac{1}{2}\left[\frac{(\frac{d\Gamma}{ds}) - (\frac{d\bar{\Gamma}}{ds})}{(\frac{d\Gamma}{ds}) + (\frac{d\bar{\Gamma}}{ds})} \pm \frac{(\frac{d\Gamma}{ds})P_i - \{(\frac{d\Gamma}{ds})P_i\}_{\Lambda_{sb}\to\Lambda_{sb}^*}}{(\frac{d\Gamma}{ds}) + (\frac{d\bar{\Gamma}}{ds})}\right], \end{aligned} \tag{30}$$

where i denotes the L, N, or T polarizations of the final state leptons. By using Eq. (16) in the above equation, the *CP* violation expression becomes

$$\mathcal{A}_{CP}(\mathbf{S}^\pm = \mathbf{e}_i^\pm) = \frac{1}{2}\left[\frac{\Delta - \bar{\Delta}}{\Delta + \bar{\Delta}} \pm \frac{\Delta_i - \bar{\Delta}_i}{\Delta_i + \bar{\Delta}_i}\right], \tag{31}$$

where $\bar{\Delta} = (\Delta)_{\Lambda_{sb}\to\Lambda_{sb}^*}$, $\bar{\Delta}_i = (\Delta_i)_{\Lambda_{sb}\to\Lambda_{sb}^*}$ and

$$\mathcal{A}_{CP}(s) = \frac{\Delta - \bar{\Delta}}{\Delta + \bar{\Delta}}, \qquad \mathcal{A}_{CP}^i(s) = \frac{\Delta_i - \bar{\Delta}_i}{\Delta_i + \bar{\Delta}_i}, \tag{32}$$

so by using these definitions, normalized *CP* violation asymmetry can be written as follows:

$$\mathcal{A}_{CP}(\mathbf{S}^\pm = \mathbf{e}_i^\pm) = \frac{1}{2}[\mathcal{A}_{CP}(s) \pm \mathcal{A}_{CP}^i(s)], \tag{33}$$

where the plus sign in the second term of the above expression corresponds to L and N polarizations, whereas the negative sign is for the T polarization.

The first term in $\mathcal{A}_{CP}(s)$ in Eq. (31) is the unpolarized *CP* violation asymmetry, while the second term $\mathcal{A}_{CP}^i(s)$ is called the polarized *CP* violation asymmetry, which provides the modifications to the unpolarized *CP* violation. After some calculation, we have found the following results for $\mathcal{A}_{CP}(s)$ and $\mathcal{A}_{CP}^i(s)$:

$$\mathcal{A}_{CP}(s) = \frac{-4\mathcal{I}m(\Lambda_{sb})\Omega(s)}{2\Delta + 4\mathcal{I}m(\Lambda_{sb})\Omega(s)},$$
$$\mathcal{A}^i_{CP}(s) = \frac{-4\mathcal{I}m(\Lambda_{sb})\Omega(s)}{2\Delta + 4\mathcal{I}m(\Lambda_{sb})\Omega^i(s)}, \quad (34)$$

where $i = L, N$, or T, and the explicit expressions of $\Omega(s)$, the $\Omega^i(s)$, are given below.

$$\Omega(s) = \mathfrak{A}_1\mathcal{I}m(C_7C^*_{9Z'}) + \mathfrak{A}_2\mathcal{I}m(C^*_9C_{9Z'}),$$
$$\Omega^L(s) = \mathfrak{A}_3\{\mathcal{I}m(C_{10Z'}C^*_9) + \mathcal{I}m(C^*_{9Z'}C_{10})\},$$
$$\Omega^N(s) = \mathfrak{A}_4\mathcal{I}m(C_7C^*_{9Z'}) + \mathfrak{A}_5\{\mathcal{I}m(C_{10}C^*_{9Z'})\}, + \mathfrak{A}_6\mathcal{I}m(C^*_9C_{9Z'})$$
$$\Omega^T(s) = \frac{\beta}{2}\mathfrak{A}_6\{\mathcal{R}e(C_{10}C^*_{9Z'}) + \mathcal{R}e(C_{10Z'}C^*_9)\},$$

with

$$\mathfrak{A}_1 = \frac{64}{3m^2_{K^*}s^2}m_b[(\mathcal{H}_3\mathcal{H}_5 + \mathcal{H}_6\mathcal{H}_4)\lambda(m^2_{K^*} - m^2_B + s) + (\mathcal{H}_3\mathcal{H}_4 + \mathcal{H}_5\mathcal{H}_6)\lambda + (3\mathcal{H}_3\mathcal{H}_4 + 2\mathcal{H}_1F_1(s)\lambda)],$$
$$\mathfrak{A}_2 = \frac{32(2m_l + s)}{3m^2_{K^*}s}[2\mathcal{H}_3\mathcal{H}_6\lambda(m^2_{K^*} - m^2_B + s) + 8\mathcal{H}^2_1m^2_{K^*}s\lambda + \mathcal{H}^2_3(12m^2_{K^*}s + \lambda) + \mathcal{H}^2_6\lambda^2],$$
$$\mathfrak{A}_3 = \frac{32\beta}{3m^2_{K^*}}[2\lambda(m^2_B - m^2_{K^*} - s)\mathcal{H}_3\mathcal{H}_6 - \mathcal{H}^2_3(12m^2_{K^*}s + \lambda) - \lambda(8m^2_{K^*}s\mathcal{H}^2_1 + \lambda\mathcal{H}^2_6)],$$
$$\mathfrak{A}_4 = \frac{128\pi}{\sqrt{s}}m_lm_b\sqrt{\lambda}[F_1(s)\mathcal{H}_3 + \mathcal{H}_1\mathcal{H}_4],$$
$$\mathfrak{A}_5 = \frac{8\pi m_l\sqrt{\lambda}}{m^2_{K^*}\sqrt{s}}(\mathcal{H}_6(m^2_{K^*} - m^2_B) + \mathcal{H}_3 - 2\mathcal{H}_7) \times (\mathcal{H}_3(m^2_{K^*} - m^2_B + s) + \mathcal{H}_6\lambda),$$
$$\mathfrak{A}_6 = 128m_l\pi\sqrt{\lambda s}\mathcal{H}_1\mathcal{H}_3.$$

IV. PHENOMENOLOGICAL ANALYSIS

In this section we describe the numerical analysis for the aforementioned observables, i.e., the polarized, unpolarized direct CP violation asymmetries and the single lepton polarization asymmetries. The input parameters which we have used in the numerical calculations, such as masses of particles, lifetimes, CKM matrix elements, etc., are given in Table II, while the Wilson coefficients are displayed in Table III. For the form factors, we rely on the updated results of light cone–QCD sum rule approach [60]. The values of these form factors and all relevant fitting parameters and their related fit formulas for the decay under consideration $B \to K^*\ell^+\ell^-$ are recollected in Ref. [48].

As far as the numerical values of the Z' couplings are concerned, there are several severe constraints from different inclusive and exclusive B decays [15,48]. These numerical values of coupling parameters of Z' model are recollected in Table I, where $S1$ and $S2$ correspond to two different fittings values for B_s-$\bar{B}_s$ mixing data by the UTfit Collaboration [61].

Before starting the numerical analysis, it is better to mention again that S_{LL} and D_{LL} represent the combination of left- and right-handed couplings of Z' with the leptons and B_{sb} denotes the left-handed coupling of Z' with the quarks [see Eq. (9)], and in our numerical analysis $S_{LL} = 0$ and $D_{LL} \neq 0$ depict the situation when the new physics comes only from the modification in the Wilson coefficient C_{10}. The opposite case, $S_{LL} \neq 0$ and $D_{LL} = 0$, indicates that the new physics is present in the process under consideration due to the change in the Wilson coefficient C_9 [see Eq. (10)]. In Figs. 1–5 we have displayed the results of single lepton polarization asymmetries as a function of the square of the momentum s within the SM and in Z' model. It is important to note here that in all the graphs the solid line corresponds to the SM values of observables, while the other curves correspond to the values of observables when we include the Z' boson effects. With the help of these graphs our findings are in order.

(i) In Figs. 1(a) and 1(b), the longitudinal P_L and the normal polarization P_N asymmetries, respectively, as a function of s, are displayed in the SM and in Z' model for the case of muons as final sate leptons. To see the influence of the Z' boson, we have drawn these asymmetries with different values of chiral couplings of Z' for $S1$ and $S2$ which are listed in Table I. These figures show that both the longitudinal and normal polarization asymmetries' values are sensitive to the choice of the values of Z' couplings. It can also be noticed from these figures that the

TABLE I. The numerical values of the Z' parameters [15,61].

	$\mathcal{R}e(B_{sb}) \times 10^{-3}$	ϕ_{sb} (in degrees)	$S_{LL} \times 10^{-2}$	$D_{LL} \times 10^{-2}$
$S1$	1.09 ± 0.22	-72 ± 7	-2.8 ± 3.9	-6.7 ± 2.6
$S2$	2.20 ± 0.15	-82 ± 4	-1.2 ± 1.4	-2.5 ± 0.9

TABLE II. Default values of input parameters used in the calculations [59].

$m_B = 5.28$ GeV, $m_b = 4.28$ GeV, $m_\mu = 0.105$ GeV, $m_\tau = 1.77$ GeV, $f_B = 0.25$ GeV, $|V_{tb}V^*_{ts}| = 45 \times 10^{-3}$, $\alpha^{-1} = 137$, $G_F = 1.17 \times 10^{-5}$ GeV^{-2}, $\tau_B = 1.54 \times 10^{-12}$ sec, $m_{K^*} = 0.892$ GeV.

TABLE III. The Wilson coefficients C^μ_i at the scale $\mu \sim m_b$ in the SM [44].

C_1	C_2	C_3	C_4	C_5	C_6	C_7	C_9	C_{10}
1.107	−0.248	−0.011	−0.026	−0.007	−0.031	−0.313	4.344	−4.669

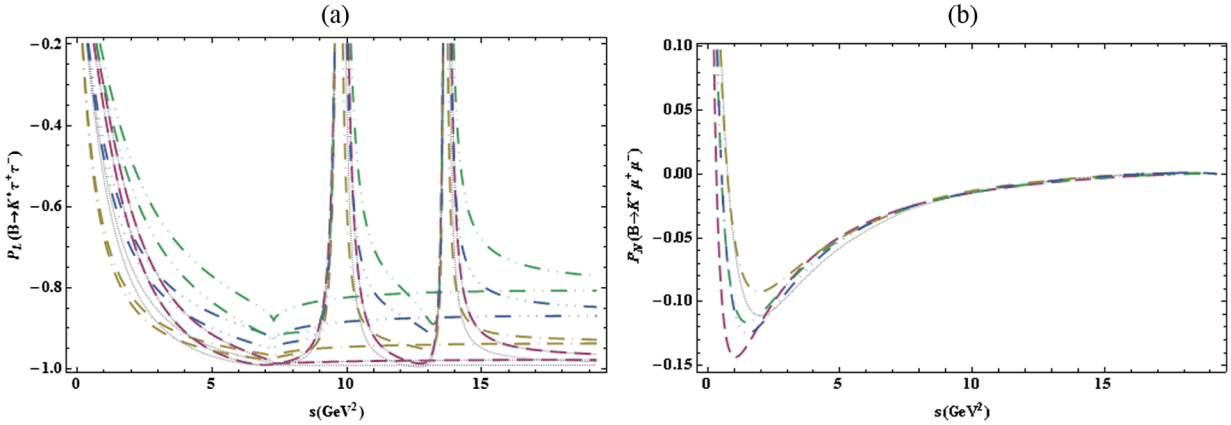

FIG. 1 (color online). (a) Longitudinal and (b) normal polarization asymmetries vs s with different values of Z' couplings in $S1$ and $S2$. The dashed line corresponds to $B_{sb} = 1.31$, $\phi_{sb} = -79°$, $S_{LL} = -6.7$, $D_{LL} = -9.3$. The dashed dotted line corresponds to $B_{sb} = 0.87$, $\phi_{sb} = -65°$, $S_{LL} = 1.1$, $D_{LL} = -4.1$. The dashed double-dotted line corresponds to $B_{sb} = 1.09$, $\phi_{sb} = -72°$, $S_{LL} = -2.8$, $D_{LL} = -6.7$. The dashed triple-dotted line corresponds to $B_{sb} = 2.05$, $\phi_{sb} = -78°$, $S_{LL} = -2.6$, $D_{LL} = -2.34$.

values of the longitudinal polarization asymmetries are sensitive throughout the s region, while for the normal polarization asymmetry the Z' effects are only prominent in the low s region and vanish for high s region. It is noted here that the transverse polarization asymmetry P_T is too tiny both in the SM and the Z' new physics.

It is important to mention here that in order to show the uncertain nonperturbative kinematical region ($7\ \text{GeV}^2 \leq s \leq 12\ \text{GeV}^2$), we have also plotted P_L with charmed resonances in Fig. 1(a). It is clear from Fig. 1(a) that in the resonance region we cannot rely on the predictions obtained just by taking into account perturbative contributions; however, one can also see from Fig. 1(a) that the effects are also well prominent and distinguished from the SM in the regions which are below ($1\ \text{GeV}^2 \leq s \leq 6\ \text{GeV}^2$) and above ($s \geq 14.4\ \text{GeV}^2$) the resonance region.

(i) We have also plotted three-dimensional graphs of P_L and P_N at $s = 3\ \text{GeV}^2$ (which is well below the resonance region) against the D_{LL} and S_{LL} in Figs. 2 and 3 for $S1$ and $S2$, respectively, for $B \to K^*\mu^+\mu^-$. From these graphs, one can clearly see the variation in the values of P_L upon varying the values of Z' couplings. For instance, from Fig. 2(a) one can extract that the SM value of P_L at $s = 3\ \text{GeV}^2$ is 0.76, which can be reduced by up to $\approx 60\%$ when we set $B_{sb} = 1.31 \times 10^{-3}$, $D_{LL} = -9.3$, and $S_{LL} = 1.1$. It is important to mention here that the values of P_L and P_N are insensitive to the value of the new weak phase ϕ_{sb}.

(ii) In Fig. 4, the longitudinal polarization of $B \to K^*\tau^+\tau^-$ is portrayed against s. Similar to the case of muons, the effects of Z' are also prominent, particularly at high values of s which are far above the resonance region. From this graph it can be seen that the maximum value of P_L which lies at s_{max} can be increased or decreased when we change the values of coupling parameters of the Z' boson. As for the previous case of muons, the value of this asymmetry is also not sensitive to the value of new weak phase ϕ_{sb}.

(iii) The normal polarization asymmetry P_N as a function of s for the case of tauons is shown in Figs. 5(a) and 5(b) for $S_{LL} = 0$ and $D_{LL} = 0$, respectively, with different values of B_{sb} and new weak phase ϕ_{sb}. We have found that P_N is an interesting observable because the Z' effects are comparatively

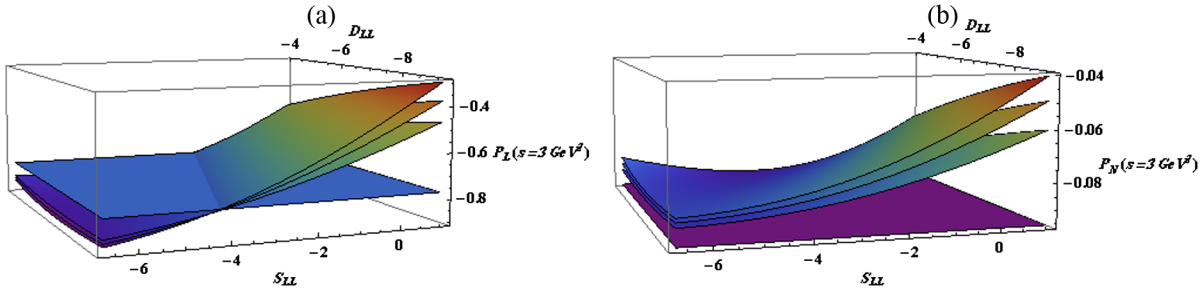

FIG. 2 (color online). Longitudinal and normal polarization asymmetries in $S1$ at $s = 3\ \text{GeV}^2$. Here the flat curves correspond to the SM values of P_L and P_N.

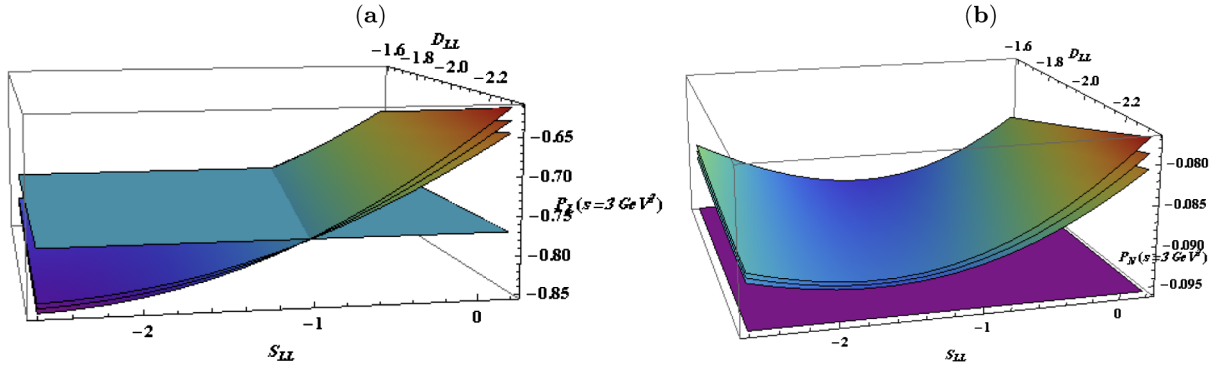

FIG. 3 (color online). Legends are the same as in Fig. 2 but for $S2$.

well prominent from the muon case [see Fig. 1(b)] throughout the available kinematical space and its value depends on the new weak phase ϕ_{sb}. Figure 5(a) depicts that due to the Z' effects, the zero crossing of the asymmetry, which lies approximately at 16 GeV^2, is shifted towards lower values of s for both $S1$ and $S2$ when we decrease the value of new weak phase ϕ_{sb}. Furthermore, the maximum value of $P_N = 0.14$ that lies at $s_{\min}$ is reduced by up to 43% when we set the value of $\phi_{sb} = -65°$. Similarly, due to the change in the value of ϕ_{sb} on setting $S_{LL} = 0$, the zero crossing of P_N is shifted left (right) for $S1$ ($S2$), as depicted in Fig. 5(b), while for the maximum value -0.14 it is increased (decreased) for $S1$ ($S2$).

The average values of asymmetries are also a very important tool for probing new physics and can be obtained by the following formula:

$$\langle P_i \rangle = \frac{\int_{4m_l^2}^{(m_B^2 - m_{k^*}^2)} P_i \frac{d\Gamma}{ds} ds}{\int_{4m_l^2}^{(m_B^2 - m_{k^*}^2)} \frac{d\Gamma}{ds} ds}. \tag{35}$$

Now we discuss the variation in the average values of

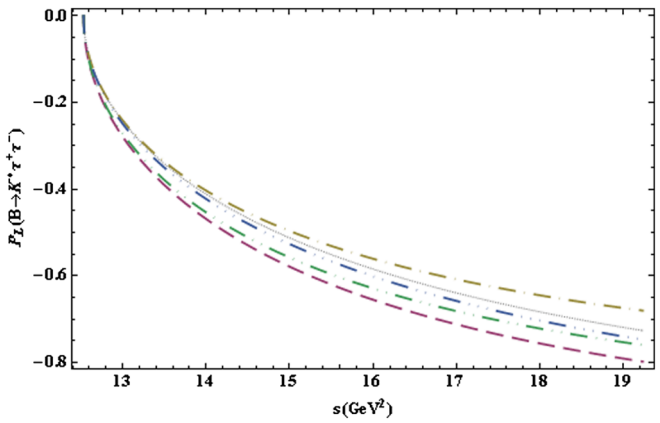

FIG. 4 (color online). Legends are the same as in Fig. 1 but for the case of $\tau^+\tau^-$.

single lepton polarization asymmetries $\langle P_i \rangle$, where $i = L$, N, or T, due to the influence of the Z' boson effect. To achieve this purpose, we have displayed $\langle P_L \rangle$, $\langle P_N \rangle$, and $\langle P_T \rangle$ in Figs. 6–11 against the different coupling parameters of Z' models. From these graphs we have found the following results:

(i) In Figs. 6 and 7 we have plotted $\langle P_L \rangle$ for the case of muons and tauons as final state leptons, respectively, as a function of S_{LL} with the different values of Z' parameters, where (a) and (b) correspond to $S1$ and $S2$. It is important to note here that the average value of P_L is not much affected due to the variation in the D_{LL} values. For this reason, we have not plotted $\langle P_L \rangle$ against D_{LL}. However, one can easily see from Figs. 6 and 7 that for the small values of S_{LL} the variation in the $\langle P_L \rangle$ is not very significant, but when we increase the value of S_{LL}, the value of $\langle P_L \rangle$ is decreased accordingly for both muon and tauons in both the scenarios $S1$ and $S2$.
On the other hand, to see the dependence of $\langle P_L \rangle$ on new weak phase ϕ_{sb}, we have listed its values with the different Z' parameters in Table IV and V for $S1$ ($S2$). From these tables, one can extract the variation in the values of $\langle P_L \rangle$ due to the change in the values of ϕ_{sb} by keeping the other parameters of Z' fixed.

(ii) For $\langle P_N \rangle$, it should be noted here that the SM value of $\langle P_N \rangle$ is $+0.01$ and due to the influence of the Z' boson, it will become too suppressed to be measured. On the other hand, the case of tauons $\langle P_N \rangle$ is displayed vs S_{LL} in Figs. 8(a) and 8(b) for $S1$ and $S2$, respectively. It is also worthwhile to mention here that similar to the case of $\langle P_L \rangle$, we have found that the value of $\langle P_N \rangle$ is mildly dependent on the value of D_{LL}. However, Figs. 8(a) and 8(b) depict that for both $S1$ and $S2$ the $\langle P_N \rangle$ crosses zero and becomes positive at a particular value of S_{LL} which shifts towards the lower value of S_{LL} when we increase the value of B_{sb}. One can also find from Figs. 8(a) and 8(b) that on setting the maximum values of Z' boson couplings, the SM value -0.021 of $\langle P_N \rangle$ is reached up to $+0.1$ ($+0.06$) for $S1$ ($S2$).

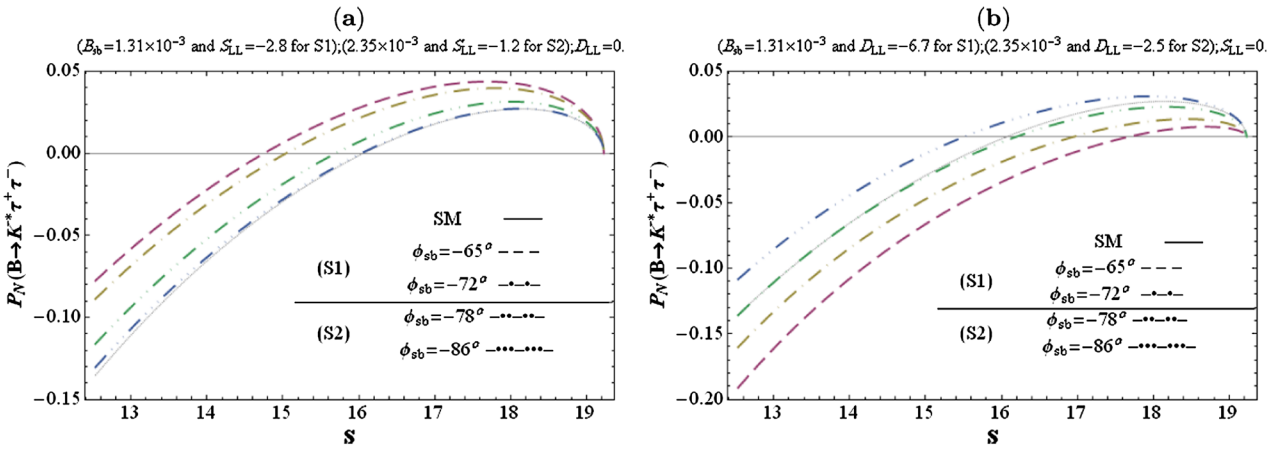

FIG. 5 (color online). Normal polarization asymmetry as a function of s (a) for $S1$ and (b) for $S2$ with different values of Z' parameters.

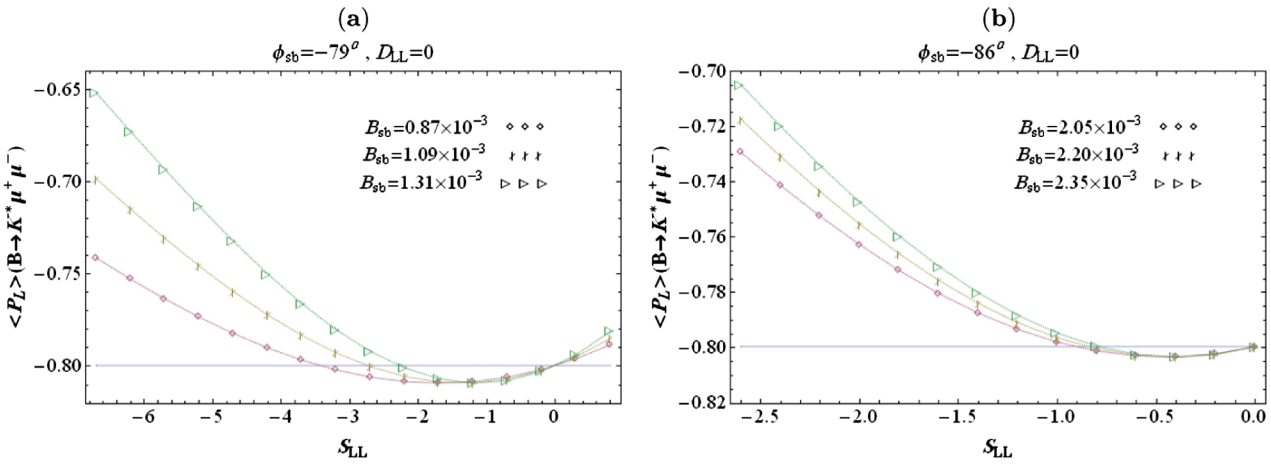

FIG. 6 (color online). Average value of the longitudinal polarization asymmetries $\langle P_L\rangle$ as a function of S_{LL} (a) in $S1$ and (b) in $S2$.

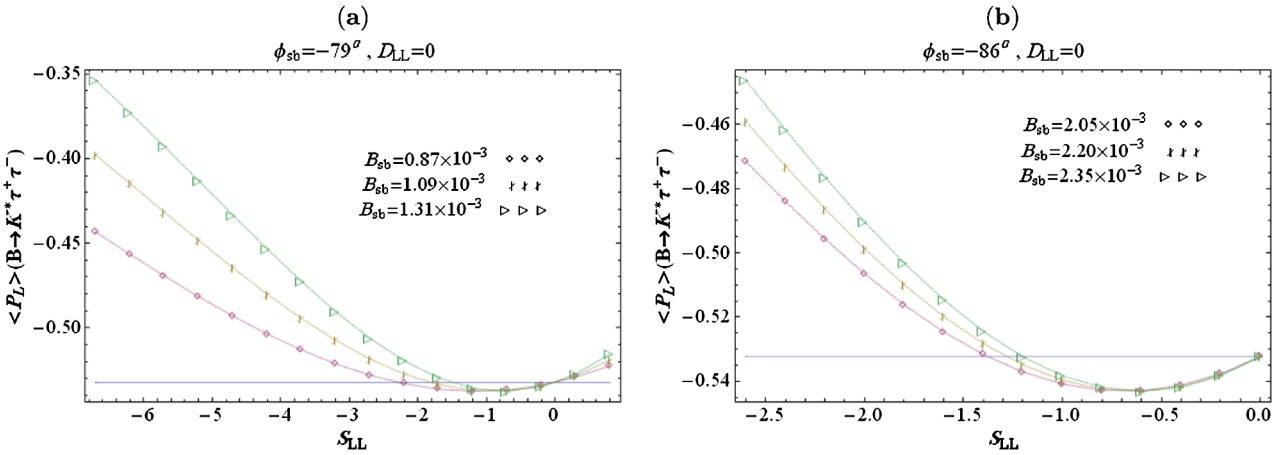

FIG. 7 (color online). Legends are the same as Fig. 6 but for $B\to K^*\tau^+\tau^-$.

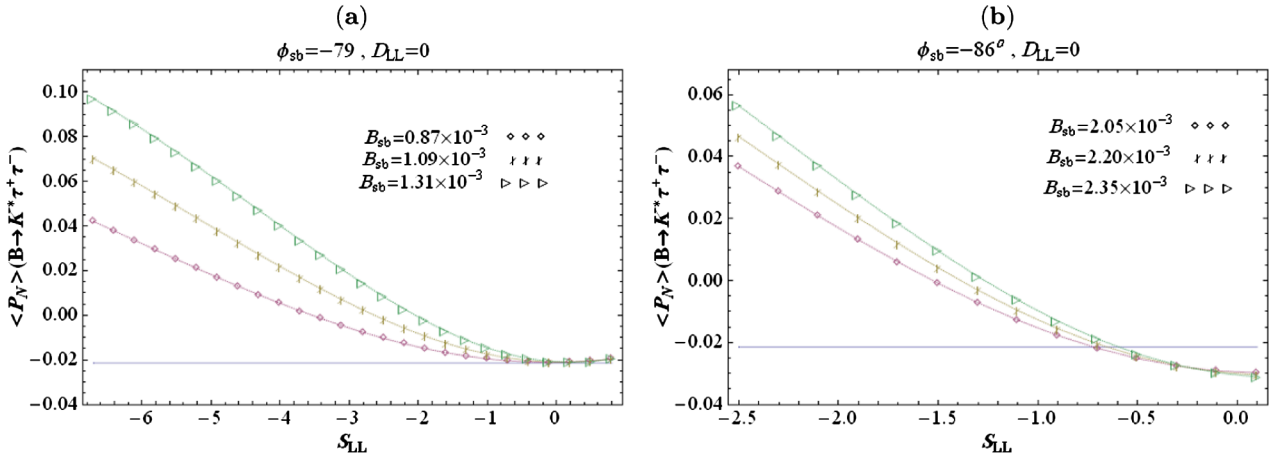

FIG. 8 (color online). The average value of normal polarization asymmetry P_N as a function of S_{LL} for $B \to K^*\tau^+\tau^-$ (a) for $S1$ and (b) for $S2$.

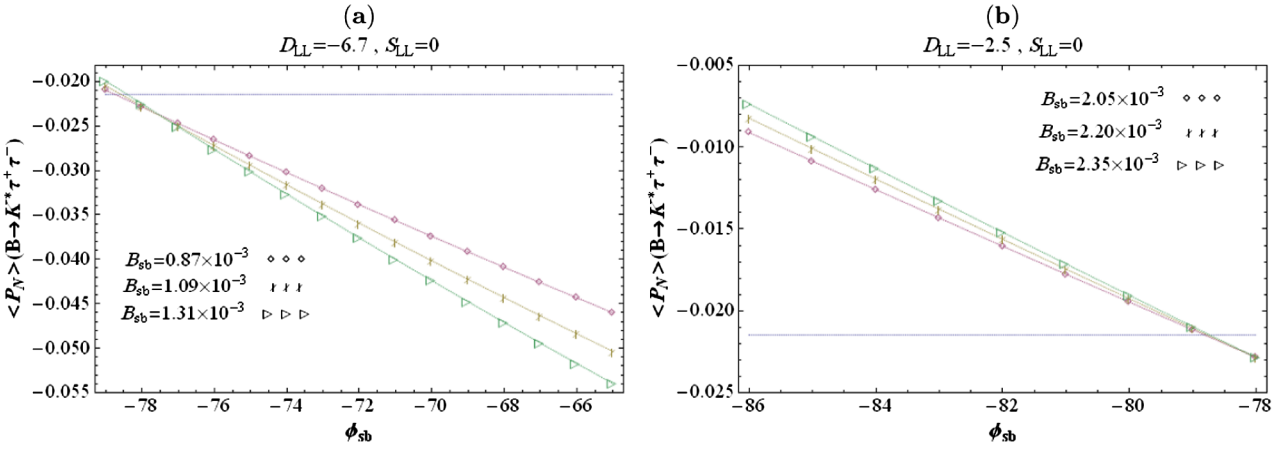

FIG. 9 (color online). Legends are the same as in Fig. 8 but as a function of ϕ_{sb}.

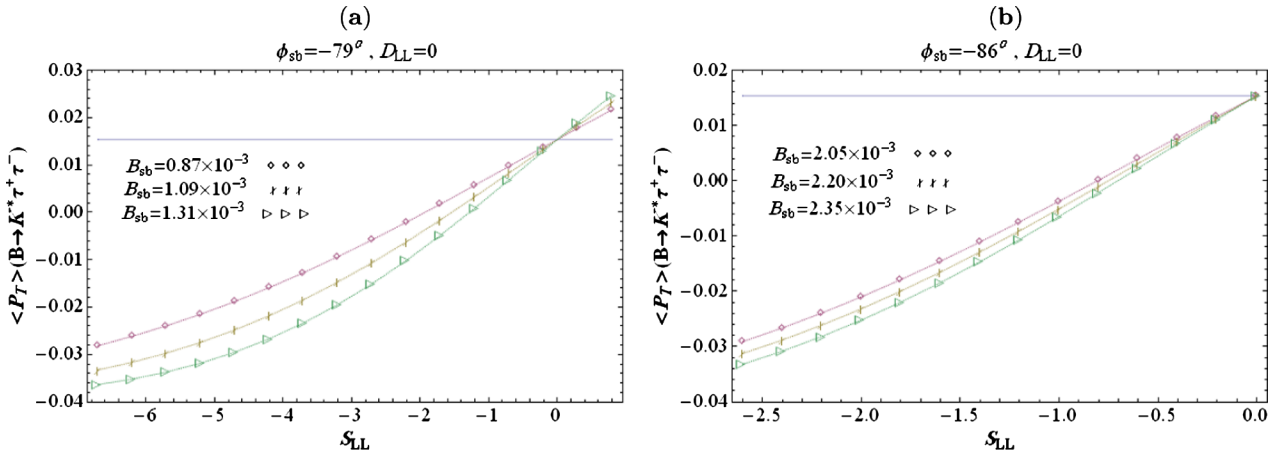

FIG. 10 (color online). Legends are the same as in Fig. 8 but for $\langle P_T \rangle$.

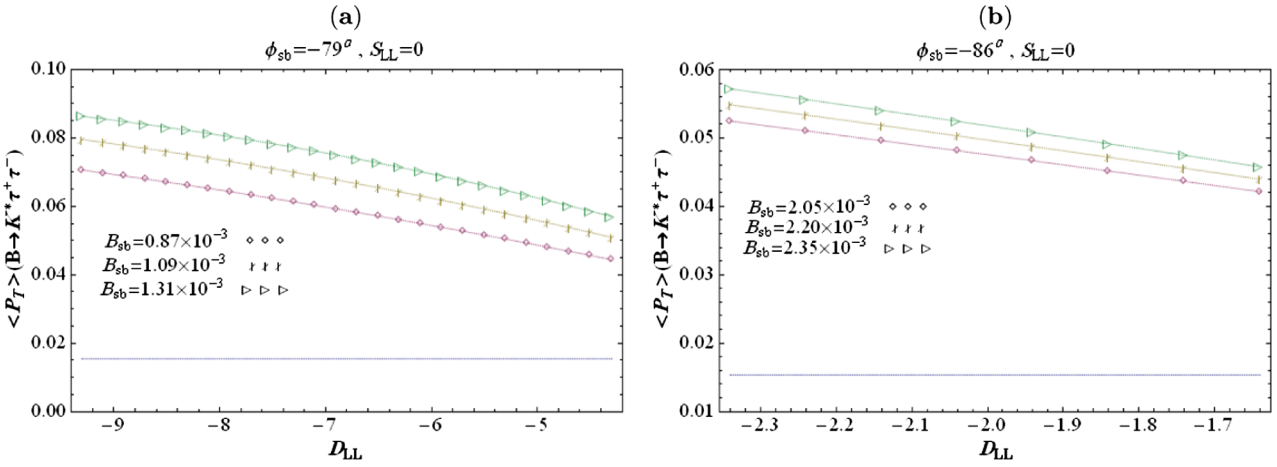

FIG. 11 (color online). The average value of transverse polarization asymmetry $\langle P_T \rangle$ as a function of D_{LL} for $B \to K^* \tau^+ \tau^-$ (a) for $S1$ and (b) for $S2$.

Therefore, the measurement of magnitude and sign of $\langle P_N \rangle$ is valuable to determine the exact values of Z' couplings.

(iii) In the same way, we have also drawn the explicit dependence of $\langle P_N \rangle$ (when tauons are the final state leptons) on ϕ_{sb} for $S1$ and $S2$ in Figs. 9(a) and 9(b), respectively, where $S_{LL} = 0$ and D_{LL} is fixed to be its central value -6.7 for $S1$ and -2.5 for $S2$. It can be easily seen from these figures that in $S1$ ($S2$) the value of $\langle P_N \rangle$ is increased (decreased) when we decrease (increase) the value of new weak phase ϕ_{sb}. For instance at $\phi_{sb} = -65^\circ$ (-86°) and $B_{sb} = 1.31 \times 10^{-3}$ (2.35×10^{-3}), the deviation in $\langle P_N \rangle$ from its SM value is about 62% (67%) for $S1$ ($S2$), while the deviation in the value of $\langle P_N \rangle$ is not significant from its SM value when we take $\phi_{sb} = -79^\circ$ (-78°). One last comment on $\langle P_N \rangle$ is that if we put $D_{LL} = 0$ and set S_{LL} to be nonzero then $\langle P_N \rangle$ is not very sensitive to the value of new weak phase ϕ_{sb}. Thus, the normal polarization asymmetry when the tauons are the final state lepton is an interesting observable to constrain the Z' boson couplings as well as to determine the accurate value of new weak phase ϕ_{sb}.

(iv) Average transverse polarization asymmetry $\langle P_T \rangle$ is depicted in Figs. 10 and 11 only for $B \to K^* \tau^+ \tau^-$ since for the case of muons, its SM value is too tiny to be measured and does not become large enough to reach the visible range due to the influence of Z' boson contribution. In contrast to the cases of $\langle P_L \rangle$ and $\langle P_N \rangle$, which are mildly effected by the variation in the value of D_{LL}, we have found that the value of $\langle P_T \rangle$ is sensitive to D_{LL}. Therefore, we have also shown the explicit dependence of $\langle P_T \rangle$ on D_{LL} in Fig. 11 along with the S_{LL} dependence, which is shown in Fig. 10. One immediate look at these figures tells us that although the dependence of $\langle P_T \rangle$ on D_{LL} is not as strong as on S_{LL}, it is significant enough to be observed. Furthermore, $\langle P_T \rangle$ is an increasing function of D_{LL} throughout the allowed region of D_{LL} for both $S1$ and $S2$. On the other hand for S_{LL}, the $\langle P_T \rangle$ behavior is approximately similar to the $\langle P_N \rangle$ case but with the opposite sign which we have discussed above. However, $\langle P_T \rangle$ is insensitive to the new weak phase ϕ_{sb}.

Now we turn our attention to analysis of another interesting observable, i.e., *CP* violation. As we have mentioned earlier in the introduction, for the $b \to s\ell^+\ell^-$

TABLE IV. Numerical values of $\langle P_L \rangle$ in Z' model for scenario I

		$\langle P_L \rangle$ at $D_{LL} = 0$				$\langle P_L \rangle$ at $S_{LL} = 0$			
		S_{LL} -6.7		S_{LL} 1.1		D_{LL} -9.3		D_{LL} -4.1	
ϕ_{sb} in degrees	Decay channel	$B_{sb} = 0.87$	1.31	0.87	1.31	0.87	1.31	0.87	1.31
-65°	$B \to K^* \mu^+ \mu^-$	-0.785	-0.715	-0.774	-0.757	-0.597	-0.485	-0.731	-0.679
	$B \to K^* \tau^+ \tau^-$	-0.423	-0.347	-0.526	-0.519	-0.515	-0.476	-0.538	-0.532
-79°	$B \to K^* \mu^+ \mu^-$	-0.741	-0.651	-0.782	-0.772	-0.573	-0.442	-0.728	-0.669
	$B \to K^* \tau^+ \tau^-$	-0.443	-0.354	-0.517	-0.506	-0.454	-0.394	-0.509	-0.490

TABLE V. Numerical values of $\langle P_L \rangle$ in Z' model for scenario II.

		$\langle P_L \rangle$ at $D_{LL} = 0$				$\langle P_L \rangle$ at $S_{LL} = 0$			
		S_{LL}		S_{LL}		D_{LL}		D_{LL}	
		-2.6		0.2		-2.34		-1.6	
ϕ_{sb} in degrees	Decay channel	$B_{sb} = 2.05$	2.35	2.05	2.35	2.05	2.35	2.05	2.35
$-65°$	$B \to K^* \mu^+ \mu^-$	-0.795	-0.780	-0.790	-0.788	-0.696	-0.675	-0.539	-0.537
	$B \to K^* \tau^+ \tau^-$	-0.437	-0.451	-0.531	-0.531	-0.535	-0.532	-0.539	-0.537
$-79°$	$B \to K^* \mu^+ \mu^-$	-0.754	-0.733	-0.793	-0.792	-0.689	-0.665	-0.736	-0.722
	$B \to K^* \tau^+ \tau^-$	-0.458	-0.434	-0.527	-0.526	-0.496	-0.488	-0.511	-0.507

transition, the value of CP violation is negligible and any measurement of this observable is a clear sign of new physics. However, we have found that both the polarized and unpolarized CP violation asymmetries for $B \to K^* \mu^+ \mu^-$ are suppressed in the SM and in Z' model. Similarly, CP violation when one of the final state tauons is transversely polarized is also found to be suppressed and, therefore, we do not include these asymmetries in our numerical discussion. The other CP asymmetries $\mathcal{A}_{CP}$ and $\mathcal{A}_{CP}^i$ (where $i = L, N$) for $B \to K^* \tau^+ \tau^-$ are displayed in Figs. 12–15, and their analysis is given in the following points.

(i) We have found that the value of direct unpolarized CP violation asymmetry $\mathcal{A}_{CP}$ is not significantly changed when we change the values of new weak phase ϕ_{sb} and D_{LL} but strongly depend on the value

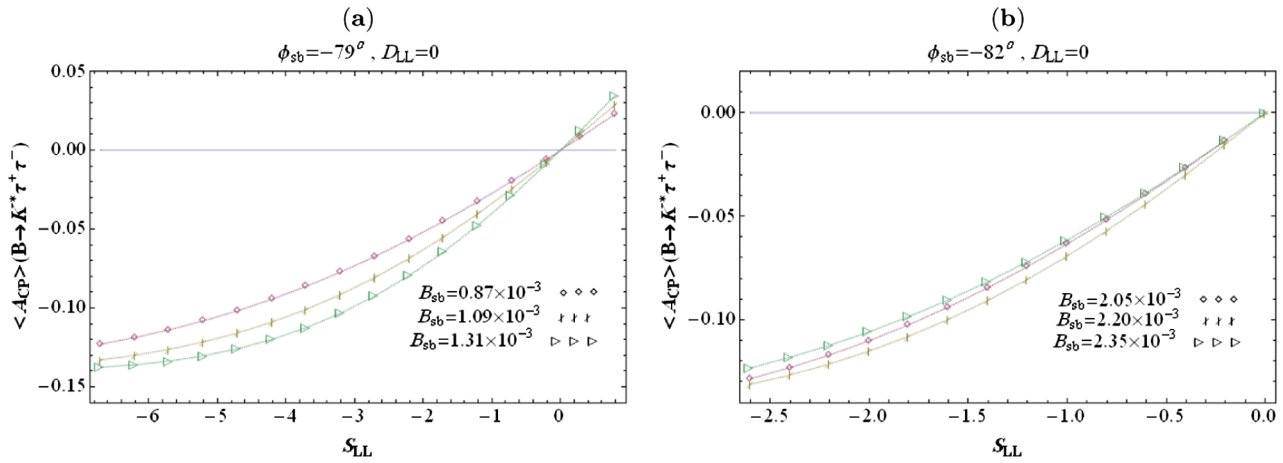

FIG. 12 (color online). Unpolarized CP violation asymmetry $\mathcal{A}_{CP}$ as function of S_{LL} for $B \to K^* \tau^+ \tau^-$ (a) for $S1$ and (b) for $S2$.

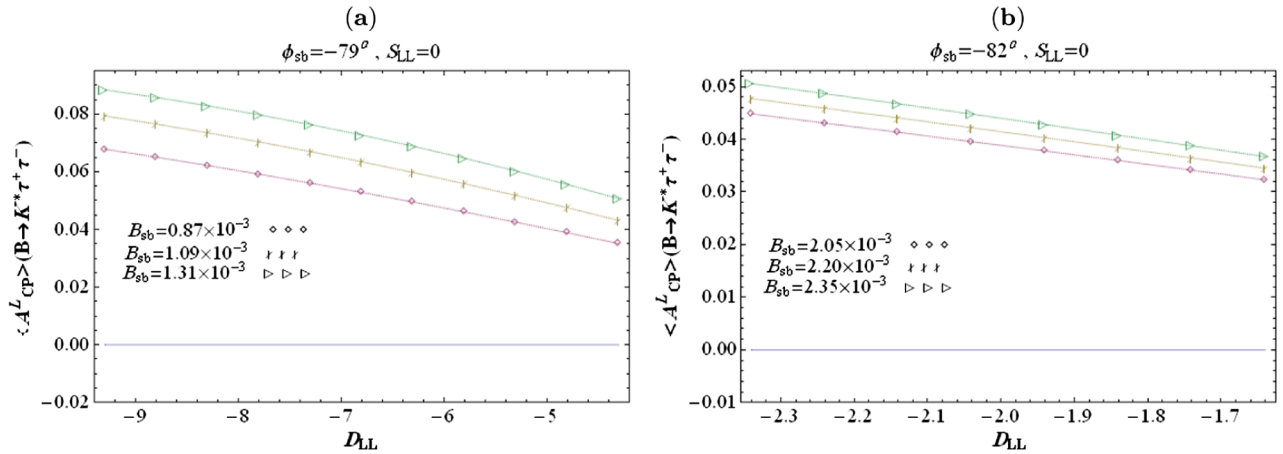

FIG. 13 (color online). Longitudinally polarized CP violation asymmetry $\mathcal{A}_{CP}^L$ as a function of D_{LL} for $B \to K^* \tau^+ \tau^-$ (a) for $S1$ and (b) for $S2$.

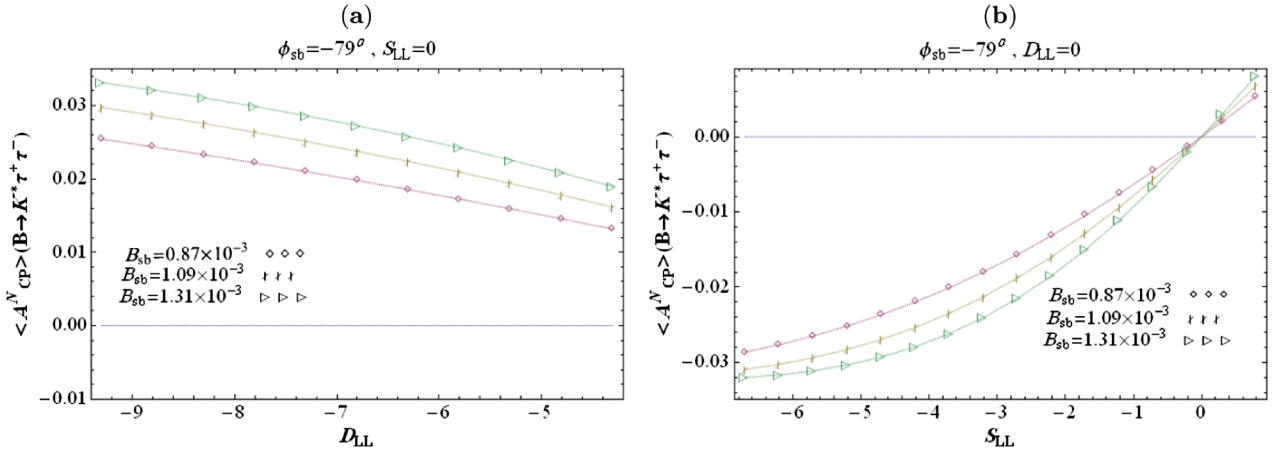

FIG. 14 (color online). Normally polarized *CP* violation asymmetry for $B \to K^*\tau^+\tau^-$ in $S1$ (a) as a function of D_{LL} (b) as a function of S_{LL}.

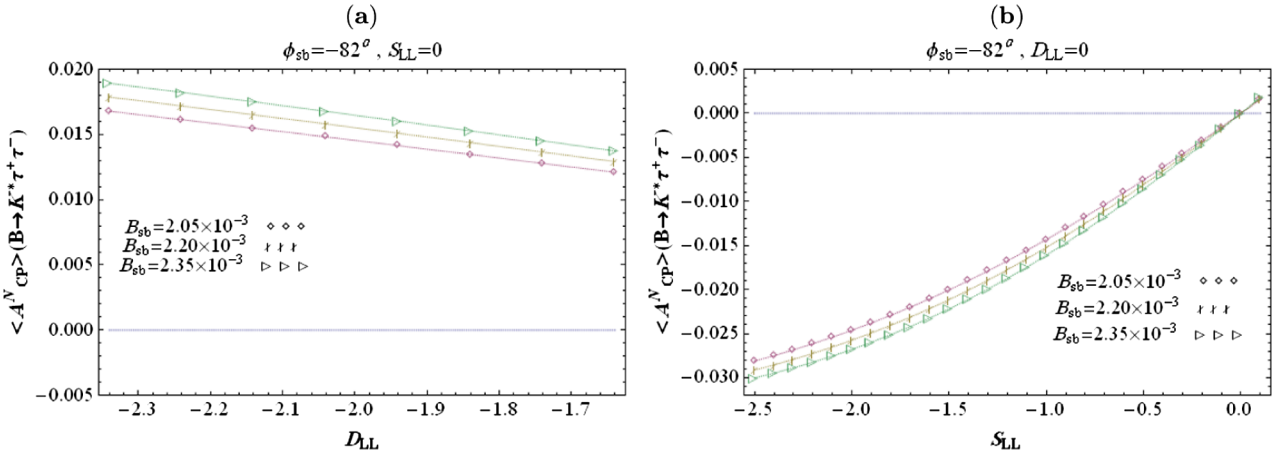

FIG. 15 (color online). Legends are the same as in Fig. 14 but for $S2$.

of S_{LL} and mildly depend on B_{sb}, as can be seen from Figs. 12(a) and 12(b) for $S1$ and $S2$, respectively. It is also noted from these figures that for both $S1$ and $S2$ the $\mathcal{A}_{CP}$ is an increasing function of S_{LL}.

(ii) The longitudinally polarized *CP* asymmetry $\mathcal{A}^L_{CP}$ is drawn in Figs. 13(a) and 13(b) for $S1$ and $S2$, respectively. In contrast to the $\mathcal{A}_{CP}$, it is found that the $\mathcal{A}^L_{CP}$ is almost insensitive to the value of S_{LL} but sensitive to the values of D_{LL} and B_{sb}. It is also important to point out here that similar to the case of $\mathcal{A}_{CP}$, the value of $\mathcal{A}^L_{CP}$ is very mildly affected due to change in the value of ϕ_{sb}. Furthermore, the value of $\mathcal{A}^L_{CP}$ is increased with the increment in the values of D_{LL} and B_{sb}. For instance, from a closer look at Fig. 13(a) one can extract that at $B_{sb} = 0.87 \times 10^{-3}$ and $D_{LL} = -4.1$ the value of $\mathcal{A}^L_{CP}$ is approximately 0.035, which is enhanced up to 0.09 when we set $B_{sb} = 1.31 \times 10^{-3}$ and D_{LL} to be -9.3.

(iii) In contrast to $\mathcal{A}_{CP}$ and $\mathcal{A}^L_{CP}$, the $\mathcal{A}^N_{CP}$ is sensitive for both S_{LL} and D_{LL}. The behavior of $\mathcal{A}^N_{CP}$ as a function of S_{LL} and D_{LL} is depicted in Figs. 14(a), 14(b), 15(a), and 15(b), respectively, for $S1$ and $S2$. These figures show that the value of $\mathcal{A}^N_{CP}$ is positive when we put $S_{LL} = 0$ and negative when we put $D_{LL} = 0$; however, in both cases, the $\mathcal{A}^N_{CP}$ is an increasing function of S_{LL} and D_{LL}.

V. SUMMARY AND CONCLUSION

In this manuscript we have analyzed the influence of nonuniversal Z' model to the $B \to K^*\ell^+\ell^-$ decay. For this purpose we have calculated *CP* violation and single lepton polarization asymmetries. To calculate the numerical values of these observables, we rely on the light cone-QCD sum rules form factors which are given in Ref. [60]. As we have mentioned in the introduction, the *CP* asymmetries for $b \to s\ell^+\ell^-$ are very tiny to be measurable experimentally, so, their measurements at current colliders would be a clear indication of NP. In this context, the unpolarized and polarized *CP* violation asymmetries are calculated for the aforementioned decay channel in Z' model. It is found that

in this model the CP violation asymmetries $\mathcal{A}_{CP}$, $\mathcal{A}_{CP}^{L}$, and $\mathcal{A}_{CP}^{N}$ are considerably enhanced for the case when tauons are the final state leptons, while for the case of muons, CP asymmetries remain suppressed. It is also found that the unpolarized CP violation is not sensitive to the D_{LL} while its value is decreased when we increase the value of S_{LL} coupling of Z'. In contrast to the unpolarized CP violation, the longitudinally polarized CP violation $\mathcal{A}_{CP}^{L}$ is not very sensitive to the S_{LL} but it is sensitive to other couplings and, similar to the case of unpolarized CP violation asymmetry, its value is also increased when we increase the values of the couplings. On the other hand, the value of $\mathcal{A}_{CP}^{N}$ is sensitive for all the couplings present in Z' model. However, the dependence of these CP asymmetries on the value of new weak phase ϕ_{sb} is very mild.

Apart from the CP violation asymmetries, the single lepton polarization asymmetries are also analyzed in the presence of the Z' boson. It is shown in this study that the values of P_i and $\langle P_i \rangle$ significantly deviate from their SM values where one can fix the parameters of Z' model. It is also shown that the longitudinal polarization asymmetry for both muons and tauons and the normal polarization only for tauons are sensitive to the new weak phase ϕ_{sb}. Therefore, the behavior of single lepton polarization asymmetries under the presence of the Z' boson depicts that precise measurements of these asymmetries may help to yield the accurate values of new weak phase ϕ_{sb} and its coupling with the fermions.

Finally, to measure the asymmetries of order 0.01 relative to the branching ratio of order 10^{-6} at 3σ level needs approximately 10^{10} to 10^{11} $B\bar{B}$ pairs (see last reference of Ref. [58]) and in LHC 10^{8} to 10^{12} $B\bar{B}$ pairs are expected to be produced. Henceforth, the precise measurements of both the CP violation and lepton polarization asymmetries for $B \to K^{*}\ell^{+}\ell^{-}$ would seem to be possible at LHC, which is a very promising and handy tool to extract out the imprints of the Z' boson at low energy level.

[1] M. S. Alam *et al.* (CLEO Collaboration), Phys. Rev. Lett. **74**, 2885 (1995).
[2] A. Barate *et al.* (ALEPH Collaboration), Phys. Lett. B **429**, 169 (1998).
[3] T. Asltonen *et al.* (CDF Collaboration), CDF Note No. CDF/PHYS/BOTTOM/CDFR/9878, 2009; V. M. Abazov *et al.* (DØ Collaboration), DØ Note No. 5928-CONF, 2009.
[4] B. Aubert *et al.* (*BABAR* Collaboration), Phys. Rev. Lett. **91**, 171802 (2003).
[5] K. F. Chen *et al.* (Belle Collaboration), Phys. Rev. Lett. **91**, 201801 (2003).
[6] B. Aubert *et al.* (*BABAR* Collaboration), Phys. Rev. D **79**, 031102 (2009).
[7] V. M. Abazov *et al.* (The DØ Collaboration), Phys. Rev. D **82**, 032001 (2010).
[8] N. Arkani-Hamed, A. G. Cohen, E. Katz, and A. E. Nelson, J. High Energy Phys. 07 (2002) 034.
[9] S. Chang and H. J. He, Phys. Lett. B **586**, 95 (2004).
[10] T. Appelquist, H. C. Cheng, and B. A. Doberscu, Phys. Rev. D **64**, 035002 (2001).
[11] C. Csaki, Mod. Phys. Lett. A **11**, 599 (1996).
[12] P. Langacker and M. Plumacher, Phys. Rev. D **62**, 013006 (2000); P. Langacker, Rev. Mod. Phys. **81**, 1199 (2009).
[13] P. Frampton, P. Hung, and M. Sher, Phys. Rep. **330**, 263 (2000).
[14] V. Barger, L. Everett, J. Jiang, P. Langacker, T. Liu, and C. Wagner, Phys. Rev. D **80**, 055008 (2009); J. High Energy Phys. 12 (2009) 048.
[15] Q. Chang, X. Q. Li, and Y. D. Yang, J. High Energy Phys. 02 (2010) 082.
[16] V. Barger, C. W. Chiang, P. Langacker, and H. S. Lee, Phys. Lett. B **598**, 218 (2004); first reference in Ref. [46].
[17] T. M. Aliev, V. Bashiry, and M. Savci, Eur. Phys. J. C **35**, 197 (2004).
[18] T. M. Aliev, V. Bashiry, and M. Savci, Phys. Rev. D **72**, 034031 (2005).
[19] T. M. Aliev, V. Bashiry, and M. Savci, J. High Energy Phys. 05 (2004) 037.
[20] T. M. Aliev, V. Bashiry, and M. Savci, Phys. Rev. D **73**, 034013 (2006).
[21] T. M. Aliev, V. Bashiry, and M. Savci, Eur. Phys. J. C **40**, 505 (2005).
[22] C.-H. Chen and C. Q. Geng, Phys. Lett. B **516**, 327 (2001).
[23] V. Bashiry, Chin. Phys. Lett. **22**, 2201 (2005).
[24] W. S. Hou, R. S. Willey, and A. Soni, Phys. Rev. Lett. **58**, 1608 (1987); **60**, 2337(E) (1988).
[25] T. Hattori, T. Hasuike, and S. Wakaizumi, Phys. Rev. D **60**, 113008 (1999).
[26] Y. Dincer, Phys. Lett. B **505**, 89 (2001) and references therein.
[27] C. S. Huang, W. J. Huo, and Y. L. Wu, Phys. Rev. D **64**, 016009 (2001).
[28] A. K. Alok, A. Dighe, D. Ghosh, D. London, J. Matias, M. Nagashima, and A. Szynkman, J. High Energy Phys. 02 (2010) 053.
[29] A. Ali, T. Mannel, and T. Morozumi, Phys. Lett. B **273**, 505 (1991).
[30] P. Colangelo, F. De Fazio, R. Feerandes, and T. N. Pham, Phys. Rev. D **74**, 115006 (2006).
[31] A. Ahmed, I. Ahmed, M. A. Paracha, and A. Rehman, Phys. Rev. D **84**, 033010 (2011).
[32] C. W. Chiang, R. H. Li, and C. D. Lu, Chinese Phys. C **36**, 14 (2012).
[33] Q. Chang and Y.-H. Gao, Nucl. Phys. **B845**, 179 (2011); Y. Li and J. Hua, Eur. Phys. J. C **71**, 1775 (2011).

[34] G. Buchalla, A. J. Buras, and M. E. Lautenbacher, Rev. Mod. Phys. **68**, 1125 (1996).
[35] A. J. Buras and M. Munz, Phys. Rev. D **52**, 186 (1995).
[36] A. J. Buras, M. Misiak, M. Munz, and S. Pokorski, Nucl. Phys. **B424**, 374 (1994).
[37] F. Kruger and L. M. Sehgal, Phys. Lett. **380**, 199 (1996).
[38] B. Grinstein, M. J. Savag, and M. B. Wise, Nucl. Phys. **B319**, 271 (1989).
[39] G. Cella, G. Ricciardi, and A. Vicere, Phys. Lett. B **258**, 212 (1991).
[40] C. Bobeth, M. Misiak, and J. Urban, Nucl. Phys. **B574**, 291 (2000).
[41] H. H. Asatrian, H. M. Asatrian, C. Grueb, and M. Walker, Phys. Lett. B **507**, 162 (2001).
[42] M. Misiak, Nucl. Phys. **B393**, 23 (1993); **B439**, 461(E) (1995).
[43] T. Huber, T. Hurth, and E. Lunghi, arXiv:0807.1940.
[44] A. Ali, P. Ball, L. T. Handoko, and G. Hiller, Phys. Rev. D **61**, 074024 (2000).
[45] W. Altmannshofer, P. Ball, A. Bharucha, A. J. Buras, D. M. Straub, and M. Wick, J. High Energy Phys. 01 (2009) 019.
[46] K. Cheung, C.-W. Chiang, N. G. Deshpande, and J. Jiang, Phys. Lett. B **652**, 285 (2007); C. H. Chen and H. Hatanaka, Phys. Rev. D **73**, 075003 (2006); C. W. Chiang, N. G Deshpande, and J. Jiang, J. High Energy Phys. 08 (2006) 075.
[47] V. Berger, C.-W. Chiang, P. Langacker, and H.-S. Lee, Phys. Lett. B **580**, 186 (2004); V. Berger, L. Everett, J. Jiang, P. Langacker, T. Liu, and C. Wagner, Phys. Rev. D **80**, 055008 (2009); R. Mohanta and A. K. Giri, Phys. Rev. D **79**, 057902 (2009); J. Hua, C. S. Kim, and Y, Li, Eur. Phys. J. C **69**, 139 (2010).
[48] Q. Chang, X. Q. Li, and Y. D. Yang, J. High Energy Phys. 05 (2009) 056; 04 (2010) 052.
[49] A. K. Alok, A. Datta, A. Dighe, M. Duraisamy, D. Ghosh, and D. London, J. High Energy Phys. 11 (2011) 121.
[50] F. Kruger and E. Lunghi, Phys. Rev. D **63**, 014013 (2000).
[51] A. Ali, E. Lunghi, C. Greub, and G. Hiller, Phys. Rev. D **66**, 034002 (2002).
[52] A. Ghinculov, T. Hurth, G. Isidori, and Y. P. Yao, Eur. Phys. J. C **33**, s288 (2004).
[53] D. Melikhov and B. Stech, Phys. Rev. D **62**, 014006 (2000).
[54] C. Chen and C. Q. Geng, Nucl. Phys. **B636**, 338 (2002).
[55] S. Fukae, C. S. Kim, and T. Yoshikawa, Phys. Rev. D **61**, 074015 (2000).
[56] W. Bensalem, D. London, N. Sinha, and R. Sinha, Phys. Rev. D **67**, 034007 (2003).
[57] K. S. Babu, K. R. S. Balaji, and I. Schienbein, Phys. Rev. D **68**, 014021 (2003).
[58] T. M. Aliev, V. Bashiry, and M. Savci, Eur. Phys. J. C **31**, 511 (2003); V. Bashiry, Phys. Rev. D **77**, 096005 (2008); V. Bashiry, N. Shrikhanghah, and K. Zeynali, Phys. Rev. D **80**, 015016 (2009).
[59] K. Nakamura *et al.* (Particle Data Group), J. Phys. G **37**, 075021 (2010).
[60] P. Ball and R. Zwicky, Phys. Rev. D **71**, 014029 (2005).
[61] M. Bona *et al.* (UTfit Collaboration), PMC Phys. A **3**, 6 (2009); M. Bona *et al.*, arXiv:0906.0953.